

The key role of interband transitions in hot-electron-modulated TiN films

S. ROTTA LORIA⁽¹⁾, A. SCHIRATO⁽¹⁾⁽²⁾, B. R. BRICCHI⁽³⁾, L. MASCARETTI⁽⁴⁾,
A. LI BASSI⁽³⁾⁽⁵⁾, M. ZAVELANI-ROSSI⁽³⁾⁽⁶⁾ and G. DELLA VALLE⁽¹⁾⁽⁶⁾⁽⁷⁾

⁽¹⁾ *Dipartimento di Fisica, Politecnico di Milano - Milano, Italy*

⁽²⁾ *Istituto Italiano di Tecnologia - Genova, Italy*

⁽³⁾ *Dipartimento di Energia, Politecnico di Milano - Milano, Italy*

⁽⁴⁾ *Czech Advanced Technology and Research Institute, Regional Centre of Advanced Technologies and Materials, Palacký University Olomouc - Olomouc, Czech Republic*

⁽⁵⁾ *Center for Nano Science and Technology, IIT@Polimi - Milano, Italy*

⁽⁶⁾ *Istituto di Fotonica e Nanotecnologie, Consiglio Nazionale delle Ricerche - Milano, Italy*

⁽⁷⁾ *Istituto Nazionale di Fisica Nucleare, Sezione di Milano - Milano, Italy*

received 13 February 2023

Summary. — Titanium nitride (TiN) is an emerging new material in the field of plasmonics, both for its linear and nonlinear optical properties. Similarly to noble metals, like, *e.g.*, gold (Au), the giant third-order optical nonlinearity of TiN following excitation with fs-laser pulses has been attributed to the generation of hot electrons. Here we provide a numerical study of the Fermi smearing mechanism associated with photogenerated hot carriers and subsequent interband transitions modulation in TiN films. A detailed comparison with Au films is also provided, and saturation effects of the permittivity modulation for increasing pump fluence are discussed.

1. – Introduction

In the last decade, the search for plasmonic materials alternative to noble metals such as gold and silver has gained notable interest. Among others [1, 2], titanium nitride (TiN) has emerged for its refractory nature, CMOS- and bio-compatibility, lower interband losses than gold (Au) at optical frequencies, and tunable permittivity at the synthesis stage. Additionally, TiN seems very promising for ultrafast plasmonics applications thanks to its extremely short hot electron relaxation time (<100 fs) compared to more conventional plasmonic materials (typically ~ 1 ps, *e.g.*, in Au) and related nonlinear optical behaviour [1, 3]. In noble metals, hot-electrons are initially photogenerated as a non-thermal population which rapidly relaxes to a thermal one. The latter dominates

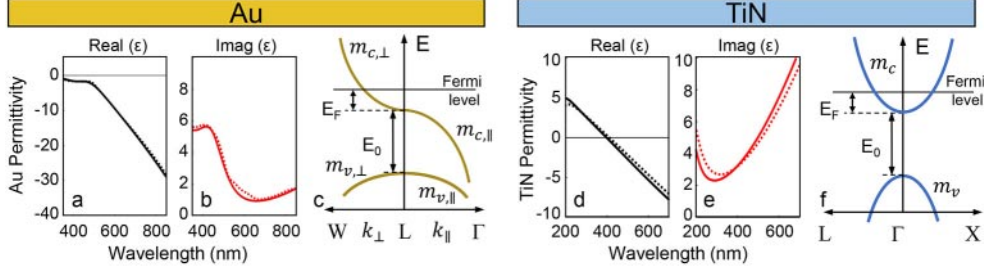


Fig. 1. – (a)–(c): Real (a) and imaginary (b) permittivity of Au at room temperature and (c) sketch of the band structure at the considered interband transition. Dotted curves in (a), (b) are experimental data from ellipsometry measurements, whereas solid curves are extracted from fitted Drude-Lorentz model. (d)–(f): Same as (a)–(c) for TiN.

the ultrafast and giant transient response via the Fermi smearing of the occupation probability in the conduction band, because of the hot-electron temperature $\Theta_e > \Theta_0$, with Θ_0 being the room temperature [4]. This effect can be interpreted as a noninstantaneous third-order optical nonlinearity [5].

In this work, we: i) Provide a Fermi smearing analysis for TiN considering one single interband transition. ii) Evaluate the subsequent permittivity modulation spectrum (real and imaginary part) as a function of the electronic temperature. iii) Provide a close comparison with Au, and reveal analogies and differences between these two plasmonic media in their nonlinear optical response.

2. – Modeling interband transition modulations

In fig. 1 we show the static dielectric permittivity and band structure for the considered interband transition of Au ((a)–(c)) and TiN ((d)–(f)). Both materials present a plasmonic character, with a negative real permittivity at optical frequencies (see figs. 1(a) and (d)). We also notice that the onset of the interband losses in TiN is blue-shifted with respect to Au (cf. figs. 1(b) and (e)). To model the static optical properties we exploit a one-Drude and one (two)-Lorentz oscillator(s) model for TiN (Au). In both cases, our simulations (solid curves) are able to reproduce the experimental data (dashed curves) with high accuracy.

Regarding Au band structure [4] (fig. 1(c)), $E_F = 0.717$ eV and $E_0 = 1.575$ eV [6], and effective masses are taken from ref. [5]. Note that, at the L point, Au exhibits a saddle in the conduction band, which is thus anisotropic, contrary to TiN that around the Γ point is assumed to be isotropic (fig. 1(f)), with $m_v = 0.72 \times m_0$, $m_c = 0.9 \times m_0$ (m_0 being the electron mass), $E_F = 0.367$ eV, and $E_0 = 2.8$ eV (in line with ref. [7]).

Following excitation with an ultrashort light pulse, and considering an instantaneous thermalization of the electron population at temperature Θ_e , we have a smearing in the electrons occupation probability around E_F . The Fermi smearing, in turn, generates a modulation of the interband transitions, with absorption being increased (reduced) for transitions to final states below (above) the Fermi level [4]. This translates to a modification of the joint density of states J_{DOS} involved in the specific transition, from which we can calculate the imaginary part of the interband permittivity modulation $\Delta\epsilon''$. For Au, under the constant matrix element approximation, we perform the calculations

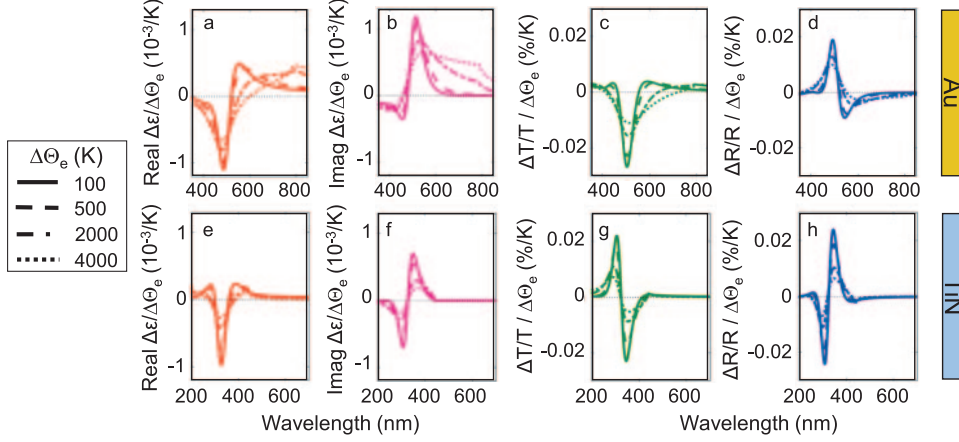


Fig. 2. – (a)–(d): Real (a) and imaginary (b) permittivity modulation spectra and corresponding differential relative transmission (c) and reflection (d) of a 30 nm thin Au film for different hot electron temperature increase $\Delta\Theta_e$, normalized to $\Delta\Theta_e$. (e)–(h): Same as (a)–(d) for a TiN film.

as in ref. [5]. In the case of TiN, we have:

$$(1) \quad \Delta\varepsilon''_{IB}(\lambda, t) = \frac{1}{12\pi\varepsilon_0} \left(\frac{e\lambda}{m_0c} \right)^2 |M|^2 \Delta J_{DOS}(\lambda, t),$$

where ε_0 is the vacuum permittivity, λ is the probe wavelength, c the light speed in vacuum and $|M|^2$ is the constant square matrix element of the transition. The real part $\Delta\varepsilon'_{IB}$ can be extracted through Kramers-Kronig transformations.

3. – Comparison between TiN and Au

The results of our calculations are displayed in fig. 2, where we considered an increasing electronic temperature variation $\Delta\Theta_e$ to study the effect of a varying pump fluence. Figure 2 shows the modulation of the real (a) and imaginary (b) part of the permittivity of Au, for different increments of the hot electron temperature. For low temperature variations, the largest values of the modulation are obtained around $\sim E_0 + E_F$. This translates to a big modulation (close to the corresponding photon wavelength, being ~ 540 nm for Au and ~ 390 nm for TiN) of the differential transmission $\Delta T/T$ (fig. 2(c)) and reflection $\Delta R/R$ (fig. 2(d)) simulated for thin films. In TiN, the modulation at low temperature increments (solid lines in figs. 2(e)–(h)) resembles the one of Au both in terms of $\Delta\varepsilon$ and subsequent $\Delta T/T$ and $\Delta R/R$. The main difference is a blue shift of ~ 200 nm of the transient spectra of TiN with respect to Au, and a different spectral shape of both $\Delta T/T$ and $\Delta R/R$, with a marked increase (decrease) in the transmission (reflection) of TiN. In the simulations of figs. 2(e)–(h), we assume $|M|^2_{\text{TiN}} \simeq 0.8|M|^2_{\text{Au}}$, as a fitting parameter to mimic an intensity peak of the $\Delta R/R$ similar to Au. The correct value of $|M|^2_{\text{TiN}}$ will be determined via a quantitative comparison with experiments, that will be the subject of a follow-up paper, in which the temporal evolution of carrier and lattice temperatures (described by a two-temperature model) is added to the description.

Further important differences arise when considering saturation effects, *i.e.*, permittivity variations for increasing hot carrier temperature change (varying pump fluence in an experiment). The fingerprint of this phenomenon is represented by the missed overlap of curves obtained at different $\Delta\Theta_e$ (normalized to $\Delta\Theta_e$). Indeed, for Au films, high saturation effects arise, with modulations getting distorted and also involving a broader spectral range. These effects have been deeply investigated in Au nanostructures and confirmed by comparison with experiments [8]. TiN modulation seems to be affected as well by the nonlinear dependence of the Fermi Dirac function on $\Delta\Theta_e$. However, nonlinearities manifest themselves mainly as a different strength of the modulation, without notable distortions of the differential spectra. The different behavior of the Fermi smearing modulation in TiN compared to Au is expected to be due to the different structure of the conduction band, which is anisotropic for Au (fig. 1). Moreover, the relative changes of the real and imaginary parts of the permittivity with respect to their static values for TiN are one order of magnitude lower than for Au (a few 10 s% vs a few 100 s%). However, a strong singularity is present for the change in TiN's $\text{Real}(\varepsilon)$ in correspondence with its ENZ feature around 400 nm.

4. – Conclusions

In conclusion, we performed a numerical study on the effect of the Fermi smearing induced in titanium nitride films by fs-laser pulses at different excitation levels. By performing an accurate comparison with Au, we noticed that the spectral spread and distortion of the response (both in terms of permittivity and of $\Delta T/T$ and $\Delta R/R$) is not found in TiN, whose dependence on the hot electron temperature increase mainly manifests as a different depth of the modulation. We propose, as a possible explanation for such discrepancy, the different conformation of the conduction band structure of the two plasmonic metals.

* * *

The authors acknowledge the METAFAST project that received funding from the European Union Horizon 2020 Research and Innovation programme under Grant Agreement No. 899673. This work reflects only author view and the European Commission is not responsible for any use that may be made of the information it contains.

REFERENCES

- [1] NAIK G. V., SHALAEV V. M. and BOLTASSEVA A., *Adv. Mater.*, **25** (2013) 3264.
- [2] SCOTOGNELLA F., DELLA VALLE G., SRIMATH KANDADA A. R., ZAVELANI-ROSSI M., LONGHI S., LANZANI G. and TASSONE F., *Eur. Phys. J. B*, **86** (2013) 154.
- [3] DIROLL B. T., SAHA S., SHALAEV V. M., BOLTASSEVA A. and SCHALLER R. D., *Adv. Opt. Mater.*, **8** (2020) 2000652.
- [4] ROSEI R., *Phys. Rev. B*, **10** (1974) 474.
- [5] MARINI A., CONFORTI M., DELLA VALLE G., LEE H., TRAN T. X., CHANG W., SCHMIDT M., LONGHI S., RUSSELL P. S. J. and BIANCALANA F., *New J. Phys.*, **15** (2013) 013033.
- [6] GUERRISI M., ROSEI R. and WINSEMIUS P., *Phys. Rev. B*, **12** (1975) 557.
- [7] ERN V. and SWITENDICK A., *Phys. Rev.*, **137** (1965) A1927.
- [8] SCHIRATO A., CROTTI G., GONÇALVES SILVA M., TELES-FERREIRA D. C., MANZONI C., PROIETTI ZACCARIA R., LAPORTA P., DE PAULA A. M., CERULLO G. and DELLA VALLE G., *Nano Lett.*, **22** (2022) 2748.